

# Effects of defected ground structure slot tuning on frequency and circuit parameters of bandpass filter

M. T. KHAN<sup>a</sup>, M. T. JILANI<sup>b</sup>, A. M. KHAN<sup>c</sup>, F. HAFEEZ<sup>d</sup>, A. M. KHAN<sup>a</sup>, A. K. MEMON<sup>a</sup>

<sup>a</sup>Department of Electrical Engineering, FEST, Indus University, Pakistan

<sup>b</sup>Graduate School of Science and Engineering, PAF Karachi Institute of Economics & Technology (PAF-KIET), Pakistan

<sup>c</sup>Department of Electronics Engineering, Sir Syed University of Engineering and Technology (SSUET), Pakistan

<sup>d</sup>Department of Electrical & Electronics Engineering, Jubail Industrial College, Saudi Arabia

In this paper the effect of the slot area to an end-coupled bandpass filter (BPF) is presented. The defected ground structure (DGS) technique is applied in the ground plane to accomplish the resonant frequency tuning of the filter. To achieve the passband the slot is designed with the etched DGS pattern consisting of two identical square-loops having open-loop edge height,  $h$  together with open-ends,  $g$  and a slot-line,  $d$  which forms connection between them. The proposed dumbbell shaped DGS is used to tune the bandpass filter down to 2.4 GHz with dimension of 40 mm × 20 mm. The gap,  $g$ , is kept constant at 0.4 mm, and  $w$  is varied. A wide tuning range of 1.31 GHz is achieved by tuning the width dimension of DGS unit cell. The improvement in center frequency, bandwidth and size of bandpass filters is achieved by the utilization of a specific DGS shape. From the analysis, it is depicted that a decrement of 25-30 % in the size of overall structure is achieved as compared to previously reported design for end-coupled bandpass filters. Meanwhile, a further decrement of 500-700 MHz in bandwidth is attained by downshifting the center frequency. Empirical modeling is achieved for frequency versus length dimensions to produce a generalized equation. With the selected structure, the filter's circuit is simulated to attain its performance corresponds to the filter's parameters setting. The results in terms of insertion and return loss, bandwidth due to the resonant frequency are presented and discussed. Effect of DGS on circuit models is also shown.

(Received January 4, 2018; accepted October 10, 2018)

*Keywords:* Bandpass filter, Circuit modeling, Empirical modeling, Frequency tuning

## 1. Introduction

In the modern era, microwave engineers are moving towards the use and implementation of frequency band above the usual high frequency (HF) and very high frequency (VHF) bands, due to broader application areas of wireless technology. The applications of microwave systems are much diversified, from entertainment to military radar applications. The problem with inaccurate standard lumped element approach, give rise to electromagnetic applications being utilized in the microwave region. The microwave region enables microwave signals to propagate over long distances through the atmosphere [1].

Emerging applications such as wireless communications continue to challenge RF/microwave filters design with ever more stringent requirements higher performance, smaller size, lighter weight, and lower cost. These filters are characterized by its bandwidth (BW), ripple in the passband (dB), the center frequency and the minimum stop-band attenuation (dB) [2].

RF and microwave bandpass filters are usually realized using transmission line structure such as microstrip, coaxial line and waveguide. The disadvantage is that such structures demand large space. Conventional microstrip filter structures are usually designed with line pieces or cascading of hi-low resistance elements. To overcome the disadvantages in the previous techniques,

many researchers moved towards the more compact and simple microstrip filter using defected ground structure (DGS) [3].

DGS is an intentionally produced defect in ground of a planar transmission line that disturbs its current distribution. Several high performance and compact components are reported by using DGS for microstrip line [4-7]. DGS unit has inherent resonant property and consequently it can be used for filter circuits. DGS provides band rejection and slow wave effect properties that can be exploited to reject unwanted frequencies and to achieve the desired compactness [8].

The integration of DGS into filter design shows a potential to control the ripple level and is able to tune the bandpass filter to a narrower bandwidth [9]. The size, harmonics suppression and efficiency of bandpass filter design can be improved with the help of proposed DGS [10-12]. Subsequently, DGS offers low circuit size and better performance in the passband as compared to the conventional bandpass filter design. DGS provides band rejection and slow wave effect properties that can be exploited to reject unwanted frequencies and to achieve the desired compactness.

The initially investigated structure is the circular head dumbbell defected ground structure [9, 13]. It is designed using a combination of two rectangular slots that is connected by a single slot in the ground plane [14, 15]. The DGS unit structure is classified according to its

different shapes. DGS unit has the property that its response can be changed by using the shape of the slot. Each DGS structure has its own distinctive characteristics based on the geometries, such functions of circuit as filtering unwanted signals and tuning high-order harmonics can easily be accomplished by means of placing required DGS patterns that correspond to the preferred circuit operations, without increasing the complexity of circuit [16]. Moreover, by varying the various dimensions of the defect the desired resonance frequency can be achieved [17].

In this paper, A modified open-end dumbbell based configuration of DGS is designed to enhance the performance of an end-coupled bandpass filter. The coupled line configuration for bandpass filter is utilized due to the requirement of a wider bandwidth of the bandpass filter. In order to achieve the desired frequency and bandwidth, bandpass filter's parameters are extracted. The parametric study of the open-loop dumbbell DGS tuning parameters of slot width is investigated for improvement of the filter characteristics. The effects of tuning parameters on the central frequency, bandwidth and RLC lumped element values are analyzed, characterized and discussed. The performance of fabricated prototype is verified by comparing its results against those obtained through the simulated (CST and ADS) results.

## 2. End coupled bandpass filter design

A modified open-end dumbbell based configuration of DGS is designed to enhance the performance of an end-coupled bandpass filter. The coupled line configuration for bandpass filter is utilized instead of stepped impedance resonator due to the requirement of a wider bandwidth of the bandpass filter. In order to achieve the desired frequency and bandwidth, bandpass filter's parameters are extracted. The width of the transmission line,  $w_s$ , permittivity and height of the substrate ( $\epsilon_r$ ,  $h_s$ ) and the open-end dumbbell DGS design parameters such as height, width and gap of the slot ( $h$ ,  $w$  and  $g$ ) are the design parameters for the bandpass filter configuration and required to be determined. Fig. 1 shows the perspective view of the design which depicts the boundary conditions and waveguide ports being used during simulation process.

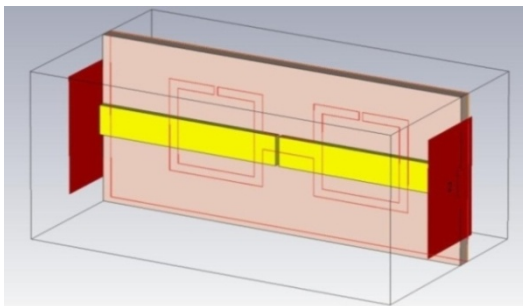


Fig. 1. Perspective view of the design

The two pole end-coupled bandpass filter is designed to operate at 2.4 GHz ISM band. EM simulation software

CST is used for design and simulation works. The designed bandpass filter uses a Rogers RT5880 substrate with a relative dielectric constant  $\epsilon_r = 2.2$  and a thickness  $h = 0.787$  mm. It has a pair of end-coupled microstrip lines with equal-length on the top and a dumbbell-shaped outline symmetrically etched in the ground plane. The  $50 \Omega$  end-coupled line has dimensions of  $L_1 = 20.8$  mm,  $w_1 = 3.5287$  mm and  $g_1 = 0.4$  mm as shown in Fig 2.

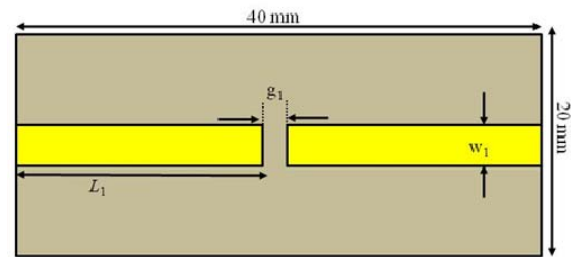


Fig. 2. Front view of the design

The etched DGS pattern consists of two identical square-loops having open-loop edge height,  $h$  together with open-ends,  $g$  and a slot-line,  $d$  which forms connection between them as depicted in Fig 3. The proposed DGS unit has dimensions of  $h = 10.25$  mm,  $d = 3.00$  mm,  $g = 0.4$  mm, and  $w = 10.25$  mm. The detail dimensions of dumbbell shaped slots and filter parameters are tabulated in Table 1. The shape and dimensions are selected for improved tuning capability (0 to 2.0 GHz) and better rejection of spurious frequencies in the passband.

Table 1. Design parameters of bandpass DGS filter

Parameter	Specification
Frequency Range	1.903 GHz – 2.829 GHz
Center Frequency, $f_0$	2.4 GHz
Bandwidth (Bw), $\Delta f$	900 MHz
Bandpass Ripple	1.0 dB max
Insertion Loss (Max)	1.0 dB max (passband)
Return Loss (Min)	10 dB min (passband)
Impedance, $Z$	50 Ohm nominal

The size of the ground plane is selected to be  $40 \times 20$  mm<sup>2</sup>. The size is optimized to provide sufficient space for the DGS to tune the end-coupled bandpass filter at required center frequency of 2.4 GHz. If the ground plane is decreased beyond the size, it produces parasitic effects leading to undesirable results. Whereas, if the ground plane is greater than the mentioned value, DGS would not radiate with it full effects [18].

The specifications of the bandpass filter design with implementation of dumbbell DGS is tabulated in Table 1. The specification is determined according to the ideal bandpass filter design.

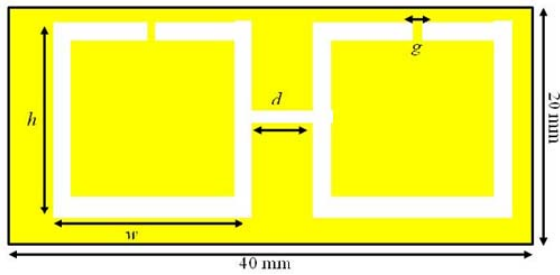


Fig. 3. Back view of the design

The requirement of desired center frequency,  $f_0$  is selected for 2.4 GHz with a minimum bandwidth of 900 MHz. A larger bandwidth is considered in the design due to the presence of end-coupled line configuration. The maximum level for passband ripple of the design is determined at -1.0 dB. The ripple level is kept to the minimum for better passband performance. The maximum insertion loss and return loss is determined at -1.0 dB and -10 dB respectively to achieve ideal bandpass characteristics of the design. The source/load impedance  $Z_0$  of 50  $\Omega$  is considered for the design in order to achieve maximum power transfer from input stage and also for maximum power transfer at the output stage of the filter.

### 3. Experimental results

Fig. 4 shows the simulated and measured results of the design. From the simulation results, it is depicted that the center resonant frequency occurs at 2.4 GHz and location of transmission zero is achieved with a zero value at DC point. It is shown that the passband is further bounded by two finite transmission-zeros at  $f_1 = 1.62$  GHz (lower transmission-zero) and  $f_2 = 2.86$  GHz (upper transmission-zero). The filter generates an insertion loss of -0.42 dB with a return loss of -12.31 dB and -3 dB bandwidth of 0.92 GHz.

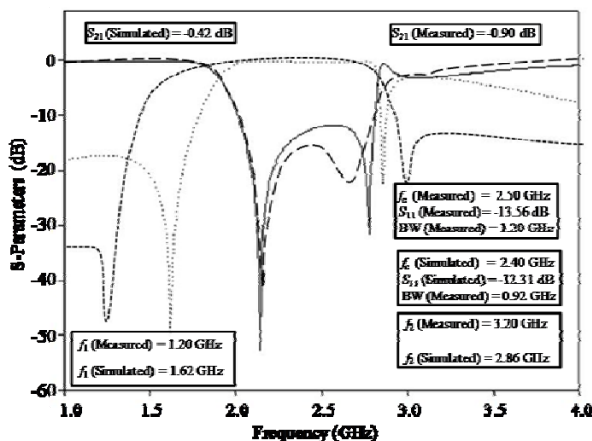


Fig. 4. Simulated and measured results for the design on RT 5880 substrate

It is also depicted that the measurement result produces a center resonant frequency of 2.5 GHz with an insertion loss of -0.905 dB, a return loss of -13.56 dB and -

3 dB bandwidth of 1.20 GHz. The location of two finite transmission-zeros occurs at frequencies of  $f_1 = 1.20$  GHz (lower transmission zero) and  $f_2 = 3.20$  GHz (upper transmission-zero). The simulated result produces a resonant frequency deviation of 0.10 GHz (4.17%), return loss deviation of -1.25 dB (10.15 %) and insertion loss deviation of -0.48 dB (53.6%) as compared to measurement results. It is observed that only small amount deviation value is produced between measured and simulated results. The result show close agreement between the fabricated and simulated results. The deviation value between the simulated and measured result could be attributed to the misalignment in the PCB fabrication of the top resonators and DGS cell on the ground plane and due to fabrication tolerance [19, 20].

The degradation between the simulated and measured result could be attributed to the mis-alignment between the top resonators and DGS [19]. The measured result almost comply the simulated result and obtained small differences in insertion loss and bandwidth due to fabrication tolerance [20].

### 4. Tuning parameters of dumbbell DGS

The resonant characteristics of the proposed bandpass filter design are mainly affected by the dumbbell DGS parameters. The dumbbell shaped DGS design parameters consists of adjustment to the dimensions of height,  $h$ , width,  $w$  and the gap,  $g$  between the slots. The geometry of the DGS design and tuning parameters of the bandpass filter is depicted in Fig. 5.

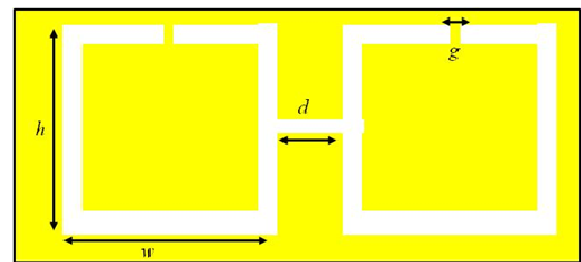


Fig. 5. Tuning parameters of the DGS design

### 5. Effect of DGS slot tuning parameters on filter characteristics

The resonant characteristics of the proposed bandpass filter design are mainly affected by the dumbbell DGS parameters. The dumbbell shaped DGS design parameters consists of adjustment to the dimensions of height,  $h$ , width,  $w$  and the gap,  $g$  between the slots. The geometry of the DGS design and tuning parameters of the bandpass filter is depicted in Fig. 5. The adjustment to the DGS structure parameters varies the value of the resonant center frequency and effective value of resistance, inductance and capacitance. The effect of width ( $w$ ), gap ( $g$ ) and height ( $h$ ) parameters on filter characteristics is discussed in the following sections.

### 5.1. Effect of varying width of the slot ( $w$ )

The first investigation involves the variation of the width ( $w$ ) of the open-loop dumbbell DGS structure. The analysis requires a change in the width of the both rectangular slot heads. The initial simulation is performed by adjusting the dimensions of width,  $w$  from 7.00 mm to 10.25 mm with an increment of 0.5 mm in every step. The result of return loss, insertion loss, frequency response and the variation of resistance ( $R$ ), inductance ( $L$ ) and capacitance ( $C$ ) values in accordance with the change in slot height is discussed and explained in the following subsections.

In this section, the effect of varying the dimensions of width  $w$  on center resonance frequency,  $f_c$  and its respective lumped element values ( $R$ ,  $L$ ,  $C$ ) are analyzed and discussed. Figs. 6 and 7 show the return loss ( $S_{11}$ ) and insertion loss ( $S_{21}$ ) plot for the result of incrementing the dimensions of  $w$  dimensions ranging from 7.0 mm to 10.25 mm with a step increment of 0.5 mm. It is recorded that the filter produces a result of return loss with values ranging from -25.00 dB to -52.38 dB. It is found that the filter response generates a good return loss level (above -10 dB) within frequency range of 2.45 GHz to 3.74 GHz. It is also observed at  $w = 7.00$  mm, the filter produces maximum return loss level of -52.38 dB. Additionally, it is depicted that the lowest frequency response of 2.45 GHz is achieved with the structure dimension of  $w = 10.25$  mm, meanwhile the highest frequency response of 3.74 GHz is observed with dimension of  $w = 7.0$  mm.

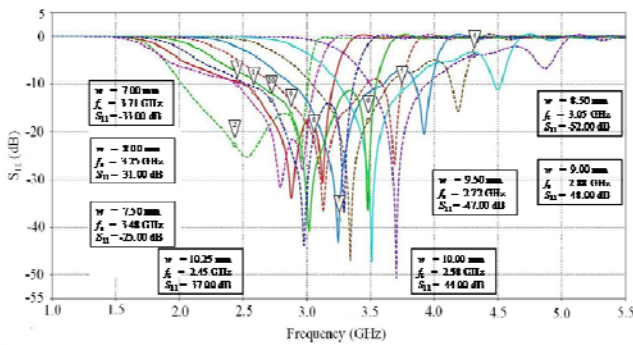


Fig. 6.  $S_{11}$  plot by adjusting both  $w$  dimensions

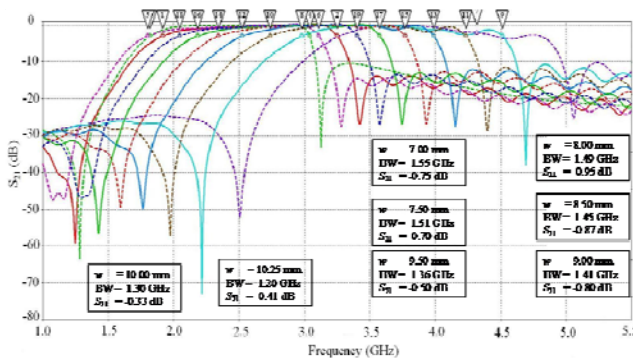


Fig. 7.  $S_{21}$  plot by adjusting both  $w$  dimensions.

The variation of center resonance frequency, resistance, inductance and capacitance with respect to  $w$  dimension ranging from 7.0 mm to 10.25 mm is tabulated

in Table 2. The equivalent lumped element values are extracted from simulated post processing of impedance analysis in CST Studio Suite.

The simulation results tabulated in Table 2 shows the variation of resistance values as the slot width,  $w$  is increased from 7.0 mm to 10.5 mm with an increment of 0.5 mm. At initial value of 7.0 mm the resistance value is 0.14  $\Omega$ . Meanwhile, at the maximum height of 10.25 mm the resistance value,  $R$  increased to 90.45  $\Omega$ . It is found that the resistance value,  $R$  is increased with the increment of slot head dimension. Consequently the value of impedance ( $Z_{11}$ , Real [ $R$ ]) for all the cases is increased from the nominal characteristic impedance of 50  $\Omega$  ranging from 77  $\Omega$  to 90  $\Omega$ . It is due to the reason that when a DGS slot is applied it increases the characteristic impedance of the transmission line causing a decrease in structure.

Meanwhile, it is also shown that the inductance value is increased from 0.78 nH to 60.25 nH as the slot width,  $w$  is increased from 7.0 mm to 10.25 mm. It is also recorded that the capacitance value is downshifted from 2.31 pF to 0.05 pF as slot width,  $w$  is increased from 7.00 mm to 10.25 mm.

Table 2. Variation of parameters due to change in  $w$  dimension

$w$ (mm)	$f_c$ (GHz)	$R$ ( $\Omega$ )	$L$ (nH)	$C$ (pF)
7.00	3.74	0.14	0.78	2.31
7.50	3.48	0.27	1.75	1.18
8.00	3.25	1.42	3.00	0.79
8.50	3.05	3.77	4.95	0.54
9.00	2.88	12.47	9.09	0.35
9.50	2.72	77.38	22.79	0.14
10.00	2.58	87.22	54.41	0.07
10.25	2.45	90.45	60.25	0.05

It is found that the results agreed with the theory of parallel RLC resonant circuit [21]. The reactance value of inductance ( $X_L = 2\pi f_L$ ) behave opposite characteristics to reactance value of capacitance ( $X_C = \frac{1}{2\pi f_C}$ ). It is also observed that capacitance value only have small variation as compared to inductance, but it produce a significant effect on the deviation of the center resonance frequency. The combination of different values of capacitance and inductance is able to provide a tuning of resonance frequency up to 1.31 GHz (2.45 GHz to 3.74 GHz).

It is also observed that as the increment of  $L$  dimension will increase the slot area. As value of inductance is decreased and consequently increased the value of capacitance [8]. It is reported that the increment of area of the DGS had decreased the center resonance frequency. The variation in structure also effects the respective values of resistance, capacitance and inductance of the resonance circuit [22, 23].

## 5.2. Mathematical formulation for the frequency tuning

The variation of the center resonance frequency with variation of slot dimension ( $w$ ) is plotted in Fig 8 using Matlab plot. The quadratic equation and polynomial values are valid for 12 iterations between the ranges of 7.00 mm to 10.50 mm as shown in Fig 8.

The Matlab Curve Fitting Toolbox is utilized to generate a mathematical formulation for the variation of DGS slot width,  $w$  with respect to center resonance frequency,  $f_c$ . Several polynomial plots had been generated by the toolbox in order to achieve a closed approximation equation for the plotted data. The polynomial equation is selected with an accuracy of above 95% as compared with input data plot. The graph is best fitted to Quadratic Polynomial equation is determined as in Equation (1).

$$f(x) = P_1 * x^2 + P_2 * x + P_3 \quad (1)$$

where,  $x$  is the dimension of  $w$  (in mm).  $P_1$ ,  $P_2$  and  $P_3$  are coefficient constants for the polynomial equation,  $f(x)$  is the corresponding frequency value at  $x$ . The value of the coefficient constants are determined as  $P_1 = -0.03692$ ,  $P_2 = -1.019$  and  $P_3 = 9.051$ .

From the input data of slot width,  $w$  (mm) and resonant frequency  $f_c$  (GHz) in Table 2, the generated polynomial equation with accuracy of above 95% is determined as in Equation (2);

$$f = -0.03692w^2 - 1.019w + 9.051 \quad (2)$$

where,  $f$  is the center frequency in GHz and  $w$  is the slot width in mm ranging from 7.00 mm to 10.25 mm. A closed approximation with accuracy of above 95% is considered for the equation. For the values or iterations more than the specified range, the polynomials  $P_1$ ,  $P_2$  and  $P_3$  values may be different.

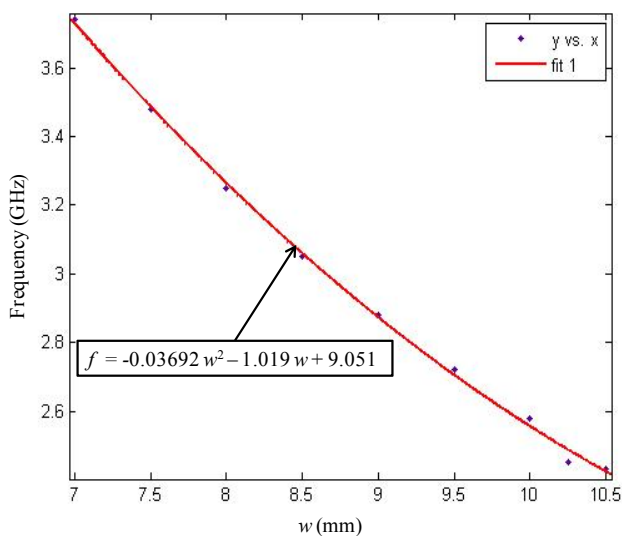


Fig. 8. curve fitting result for  $w$  (mm) against frequency (GHz)

It is concluded by the above results and discussions that dumbbell DGS provides good characteristics as compared to other type of DGS structures for bandpass filter design and tuning [9, 16]. Moreover, the resonant frequency of the dumbbell shaped DGS can be controlled by the parameters of height,  $h$  and width,  $w$ . In this study, the dimensions of dumbbell DGS are tuned to achieve the center frequency tuning of the bandpass filter which operates at center frequency of 2.50 GHz with a bandwidth of 1.2 GHz. The fabricated unit is able to suit the demands of commercial WLAN applications. Fig. 9 and 10 depicts the fabricated model of the proposed design.



Fig. 9. Fabricated bandpass filter, front view

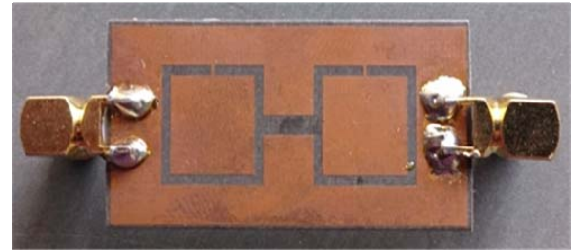


Fig. 10. Fabricated bandpass filter, back view

## 6. Effect of DGS slot tuning parameters on RLC

In order to validate the proposed design, an equivalent lumped element circuit of end-coupled line DGS bandpass filter is modeled. The step is preceded after the preliminary estimation and initial designing using CST Microwave Studio. The Advanced Design System (ADS) software is used to model the equivalent circuit of the filter design. The equivalent lumped model of the proposed bandpass filter is designed by transforming each filter component into its equivalent RLC block which represents the components of the microstrip transmission line, end-coupled line and defected ground structure (DGS). The reliability of the proposed bandpass filter equivalent lumped model and its parametric study is verified by comparing its return loss ( $S_{11}$ ) and insertion loss ( $S_{21}$ ) with simulated results that is obtained through CST design. The impedance analysis is performed with CST simulation to extract the value of resistance  $R$ , capacitance,  $C$  and inductance,  $L$  for the resonance frequency. The RLC equivalent circuit and  $S_{11}$  parameters are derived from the Z-parameters value for the corresponding center frequency.

The designed bandpass filter with integration of defected ground structure is evaluated by an LC resonant circuit. In order to model the designed bandpass filter that is presented in Section 2, it is necessary to extract the equivalent circuit parameters. The proposed equivalent circuit for an end-coupled bandpass filter with a dumbbell shaped DGS is shown in Fig 11 using Equations (3) to (6) [2]. The value of parallel capacitance  $C_p$  is determined from Equation (3) and produced a value of 0.977 pF.

$$C_p = \frac{\omega_c}{z_{0g1}(\omega_0^2 - \omega_c^2)} = \frac{5f_c}{\pi(f_0^2 - f_c^2)} \quad (3)$$

Consequently the value of parallel inductance  $L_p$  is determined as 2.644 nH from Equation (4).

$$L_p = \frac{25}{C_p(\pi f_0)^2} \quad (4)$$

where,  $f_c$ , is the cut-off frequency (GHz) of the band reject response of the slot at 3 dB and  $f_0$  is its pole frequency (GHz). At frequency  $f < f_0$ , the parallel circuit behaves as inductor and its equivalent inductance  $L_{eq}$  (nH) is given by Equation (5)

$$L_{eq} = \frac{L_p}{[1 - (\frac{f}{f_0})^2]} \quad (5)$$

Bandpass configuration is created by a coupling gap ( $g$ ) in 50  $\Omega$  microstrip line. For  $f < f_r$  (series resonance), bandpass DGS configuration behaves as capacitor. If a dumbbell structure is used in bandpass mode, its pole frequency  $f_p$  is changed by a small amount. The -3 dB frequency is assumed to be same for bandpass as for bandstop.  $f_r$  is obtained by EM simulation results. Meanwhile, the value of coupling capacitance  $C_s$  is determined from Equation (6) with a value of 0.563 pF.

$$C_s = \frac{25.33}{L_{eq}f_s^2} \quad (6)$$

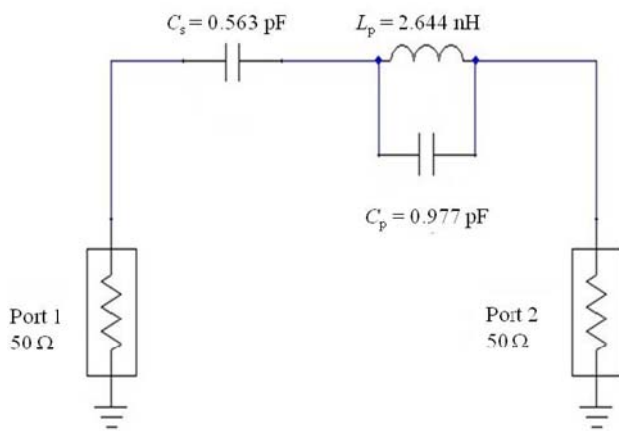


Fig. 11. Fabricated bandpass filter, front view

Table 3 illustrates the equivalent parameters for the circuit analysis of end-coupled DGS bandpass filter design

for determining  $L_p$ ,  $L_{eq}$ ,  $C_s$ ,  $C_p$ ,  $f_s$ ,  $f_p$  and  $f_c$ . It is found that the integration of DGS under microstrip line produces a resonance of the transmission line structure. The resonant characteristics of the DGS unit cell can be therefore represented with an RLC equivalent circuit.

Table 3. Equivalent circuit parameters values for the proposed end-coupled line DGS-BPF

Parameter	Specification
$L_p$	2.644 nH
$L_{eq}$	32.50 nH
$C_s$	0.563 pF
$C_p$	0.977 pF
$f_s$	3.04 GHz
$f_p$	3.13 GHz
$f_0$	2.42 GHz

The return loss ( $S_{11}$ ) and insertion loss ( $S_{21}$ ) results of end-coupled bandpass filter obtained through CST and ADS simulations are depicted in Fig 12. The return loss of -52.38 dB is achieved through CST simulation at center resonant frequency of 2.40 GHz with a bandwidth of 0.92 GHz. The ADS simulation provides the return loss of -38.25 dB at resonance frequency of 2.42 GHz with a bandwidth of 0.82 GHz. It is also found that the insertion loss of -0.42 dB is observed with CST simulation, whereas the ADS simulation generated an insertion loss of -0.25 dB. Furthermore, according to CST simulation, the bandpass filter is bounded by two transmission zeros at  $f_1 = 1.62$  GHz and  $f_2 = 2.86$  GHz. For the ADS simulation, the transmission zero is generated at  $f_1 = 3.16$  GHz.

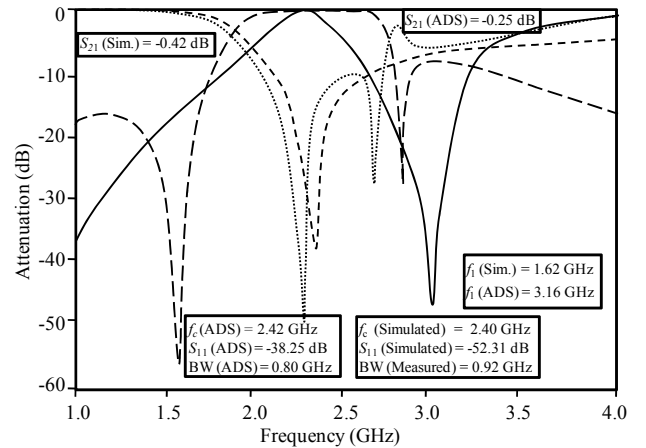


Fig. 12. Simulated and theoretical (ADS) responses for an end-coupled bandpass filter design

## 7. Conclusion

An end-coupled bandpass filter with an integration of open-loop dumbbell-shaped DGS is proposed with the size of  $40 \times 20 \text{ mm}^2$ . The bandpass filter operates at center resonant frequency of 2.50 GHz with an insertion loss of -0.905 dB, a return loss of -13.56 dB and -3 dB bandwidth of 1.2 GHz. The effects of width,  $w$  parameter of dumbbell DGS on bandpass filter characteristics are comprehensively discussed. Consequently, the designed bandpass filter is validated by extracting the equivalent circuit parameters. The proposed bandpass filters are fabricated and being implemented with the testing and measurement processes. Thus, from all measurement results it is found that the performance of the fabricated structure had been validated with comparison to the simulated results.

## References

- [1] I. Hunter, Theory and Design of Microwave Filters, Herts, United Kingdom: British Library Catalogue in Publication Data, 2001.
- [2] A. Bedair, A. Mooty, A. Rahman, Design and Development of High Gain Wideband Microstrip Antenna and DGS Filters Using Numerical Experimentation Approach, PhD, Faculty of Electrical Engineering and Information Technology, Otto-von-Guericke-Universität Magdeburg, 2005.
- [3] J. S. Hong, Microstrip Filters for RF/Microwave Applications, Hoboken, New Jersey: John Wiley & Sons, Inc., 2011.
- [4] G. Breed, High Frequency Electronics, ed. Summit Technical Media, LLC, 50 (2008).
- [5] M. S. Jung, J. S. Park, J. B. Lim, H. G. Cho, A Novel Defected Ground Structure and its Application to a Microwave Oscillator, presented at the 33<sup>rd</sup> European Microwave Conference, Munich, (2003).
- [6] L. He, L. Sun, W. Jincai, International Conference on Electronics, Communications and Control (ICECC) 2690 (2011).
- [7] Y. J. Ko, J. Y. Park, J. U. Bu, IEEE Microwave and Wireless Components Letters **13**, 276 (2003).
- [8] L. H. Weng, Y. C. Guo, X. W. Shi, X. Q. Chen, Progress In Electromagnetics Research B **7**, 173 (2008).
- [9] M. Chalal, F. Labu, M. Dehmas, A. Azhar, WSEAS Transactions on Circuits and Systems **10**, 413(2011).
- [10] D. Baatarkhuu, Y. S. Choi, S. T. Yu, T. Tharoeun, H. Liu, D. Ahn, Equivalent Circuit Model for Two Layer Dumbbell Type Defected Ground Structures, PIERS Proceedings, Suzhou, China, 2011.
- [11] D. Ahn, J. S. Park, IEEE Transaction on Microwave Theory and Techniques **49**, January (2001).
- [12] J. S. Park, J. S. Yun, D. Ahn, IEEE Transaction on Microwave Theory and Techniques **50**, 2037 (2002).
- [13] S. K. Parui, S. Das, Radio Engineering **16**, 16 (2007).
- [14] A. K. Arya, Kartikeyan, M. V. A. Patnaik, Efficiency Enhancement of Microstrip Patch Antenna with Defected Ground Structure, presented at the Recent Advances in Microwave Theory and Applications, 2008.
- [15] A. K. Arya, M. V. Kartikeyan, A. Patnaik, Neural Network Model for Analysis of DGS Structure, presented at the National Symposium on Vacuum Electronic Devices & Applications (VEDA), (2009).
- [16] Y. Chung, S. S. Jeon, S. Kim, D. Ahn, J. I. Choi, T. Itoh, IEEE Transaction on Microwave Theory and Techniques **52**, May (2004).
- [17] K. Foorooraghi, H. Dalili Oskouei, M. Hakkak, Progress In Electromagnetics Research, PIER **73**, (2007).
- [18] S. Singh, B. Rawat, DGS based SIR Filters for Wireless Communication on Anisotropic Substrate, Proceedings of Asia-Pacific Microwave Conference, Yokohama, 2006.
- [19] Y. T. Lim, K. M. Lum, A Stepped Impedance Comb-line Filter Design Using Defective Ground Structure for Wireless Applications, PIERS Proceedings, Kuala Lumpur, Malaysia, (2012).
- [20] X. Q. Chen, Y. C. Guo, X. W. Shi, Progress In Electromagnetics Research M **3**, 141 (2008).
- [21] C. Bowick, RF Circuit Design: Elsevier's Science & Technology, 1997.
- [22] A. Anand, A. Bansal, K. Shambavi, Z. C. Alex, Design and Analysis of Microstrip line with Novel Defected Ground Structure, International Conference on Advanced Nanomaterials and Emerging Engineering Technologies(ICANMEET), Chennai, 2013.
- [23] S. K. Parui, S. Das, Radio Engineering **16**, 16 (2007).

\*Corresponding author: talha.khan@indus.edu.pk